



## MOTOR INPUT VOLTAGE AND RECTIFIER FIRING ANGLE VARIATION WITH LOAD TORQUE IN CONSTANT CURRENT OPERATED INDUCTION MOTORS

Mehmet Akbaba

Electrical and Electronics Engineering Department, University of Bahrain, P.O. Box 32038, Isa Town, Kingdom of Bahrain

[akbaba@eng.uob.bh](mailto:akbaba@eng.uob.bh)

**Abstract**-In current source inverter (CSI) fed induction motors (IM) operated under constant current, the input voltage changes within large limits as the load torque changes. In such an operation the motor mostly operates on the saturated portion of its magnetizing characteristic, and non-linear relation exists between the input voltage and the load torque. Therefore in this paper a numerical technique is presented for obtaining required input voltage corresponding to a given load torque, which can be used for estimating the firing angle of the input rectifier, which in turn can be used for predicting firing angle in terms of load torque. Proposed technique has been demonstrated with an example.

**Keywords**-Constant current, firing angle, induction motor, required voltage.

### 1. INTRODUCTION

Although it is more common to operate induction motors from voltage sources, it is also common practice to operate the induction motors from current sources. Thus instead of controlling the stator voltages, the stator currents can be controlled directly to control the electromagnetic torque. Since electromagnetic torque is produced by the interaction of the magnetic flux linkages and rotor currents, an improved dynamic performance results when stator currents are controlled directly [1]. The input current source is shared between the rotor current and magnetizing current. At low slip values the rotor current is small. In this case the magnetizing current will share a large proportion of the constant stator current and hence the machine will operate under heavy saturation. For this reason a correct analysis and design of constant current operated induction motors can not be done without taking saturation into account.

In the past many research efforts have been devoted to the analysis and design of constant current operated induction motors [2-6]. However no attempt was made to determine the input voltage requirement in relation to the load torque. This information will lead to assessment of the input rectifier firing angle in relation to the load torque, which will be very useful in system analysis and design stages. The aim of this paper is to propose a methodology for this purpose and illustrate it with an application example.

### 2. MATHEMATICAL MODEL FOR DETERMINATION OF THE INPUT VOLTAGE

Schematic diagram of a constant current operated induction motors is given in Fig. 1 and constant current steady-state equivalent circuit of IM is given in Fig. 2.

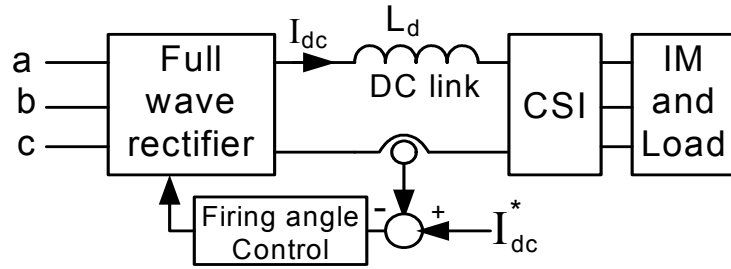


Fig. 1. Constant current control of induction motors

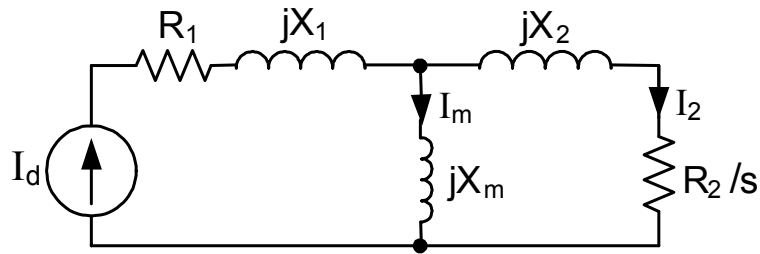


Fig. 2. Constant current operation equivalent circuit

From Fig. 1 it can be seen that in normal practice, the required firing angle of the rectifier is determined by processing of the DC link current. Alternatively the firing angle can be determined by computing the required input voltage of the motor corresponding to a given load torque, and then using well known relation between rectifier output voltage, firing angle and the motor input voltage. This last new approach is the subject to this paper.

All parameters in Fig. 2 are referred to the stator side. Iron losses are ignored.  $I_{dc}$  is the current source used for driving the motor and  $I_{dc}^*$  is the reference dc link current.

At low speeds the current controlled induction motors operate under strong magnetic saturation. To analyze the performance under such an operating condition, it is necessary to model the magnetizing characteristic of the motor. Magnetizing characteristic can be obtained either experimentally or determined from design details of the motor. In this investigation the magnetizing characteristic is modeled as:

$$\lambda_m = \frac{a_1 I_m + a_2 I_m^4}{b_1 + b_2 I_m + b_3 I_m^3 + b_4 I_m^4} \quad (1)$$

Where  $\lambda_m$  is the magnetizing flux linkages,  $I_m$  is the magnetizing current and  $a_1, a_2, b_1, b_2, b_3,$  and  $b_4$  are motor dependent coefficients. Magnetizing reactance can be calculated from Equation (1) as:

$$X_m = \omega \lambda_m / I_m \quad (2)$$

Where;  $\omega$  is the angular frequency of the supply voltage. In constant current operation it was found that the rotor leakage reactance has negligible effect on the performance of the motor. Utilizing Fig. 2 and ignoring the rotor leakage reactance, the electromagnetic torque can be written as:

$$T = \frac{3 R_{eq} X_m^2 I_d^2}{\omega_s (R_{eq}^2 + X_m^2)} \quad (3)$$

Where  $R_{eq}$  is used instead of  $R_2/s$  (where  $s$  is the per-unit slip) and it represents the unknown speed.  $\omega_s$  is the mechanical synchronous angular frequency of the shaft.

In steady-state operation the friction torque is ignored and the electromagnetic torque is assumed to be equal to the load torque  $T_L$ , i.e.,  $T=T_L$ . Therefore in the following equations  $T_L$  is used instead of  $T$ .

Utilizing Fig. 2, square of the magnetizing current can be written as:

$$I_m^2 = \frac{R_{eq}^2 I_d^2}{R_{eq}^2 + X_m^2} \quad (4)$$

Combining equations (1), (2), (3) and (4), the following two functions can be obtained for solving the unknown speed which is represented by  $R_{eq}$  and the magnetizing current.

$$Fn_1 = \omega_s T_L R_{eq}^2 + \omega^2 (\omega_s T_L - 3 I_d^2 R_{eq}) (Q_1 / Q_2) \quad (5)$$

$$Fn_2 = R_{eq}^2 [I_m^2 - I_1^2] + \omega^2 I_m^2 Q_1 / Q_2 \quad (6)$$

Where;

$$Q_1 = (a_1 + a_2 I_m^3)^2 \quad (7)$$

$$Q_2 = (b_1 + b_2 I_m + b_3 I_m^3 + b_4 I_m^4)^2 \quad (8)$$

Equations (5) and (6) are highly nonlinear and can be solved using Newton-Raphson method [7] as follows:

$$[J] \begin{bmatrix} \Delta I_m \\ \Delta R_{eq} \end{bmatrix} = - \begin{bmatrix} Fn_1(I_{m0}, R_{eq0}) \\ Fn_2(I_{m0}, R_{eq0}) \end{bmatrix} \quad (9)$$

Where,  $I_{m0}$  and  $R_{eq0}$  are the initial guesses of the magnetizing current  $I_m$  and  $R_{eq}$ .  $\Delta R_{eq}$  and  $\Delta I_m$  are the increments (or decrements) in  $I_m$  and  $R_{eq}$  after each iterations step.  $[J]$  is the Jacobian matrix of the functions given in equations (5) and (6) and it is determined as follows:

$$[J] = \begin{bmatrix} \frac{\partial F n_1(I_{m0}, R_{eq0})}{\partial I_m} & \frac{\partial F n_1(I_{m0}, R_{eq0})}{\partial R_{eq}} \\ \frac{\partial F n_2(I_{m0}, R_{eq0})}{\partial I_m} & \frac{\partial F n_2(I_{m0}, R_{eq0})}{\partial R_{eq}} \end{bmatrix} \quad (10)$$

Having computed  $\Delta I_m$  and  $\Delta R_{eq}$  from equation (9), then the two unknowns are computed as:

$$I_{m,l} = I_{m0} + \Delta I_m \quad (11)$$

$$R_{eq,l} = R_{eq0} + \Delta R_{eq} \quad (12)$$

Iterations can continue until desired accuracy is achieved. Having computed the magnetizing current and  $R_{eq}$  and the slip as  $s = R_2 / R_{eq}$ , the magnetizing reactance can be obtained from equation (2) and the speed of the motor is obtained as:

$$n = n_s (1 - s) \quad (13)$$

Where:

$n$  is the rotor speed in rpm and  $n_s$  is the rotor synchronous speed in rpm.

Finally the *rms line-to-line input voltage of the motor* is computed as:

$$V_m = \sqrt{3} Z_{in} I_d \quad (14)$$

Where  $Z_{in}$  is the input impedance of the motor, which is obtained from Fig. 2 as:

$$Z_{in} = \sqrt{\left( R_1 + \frac{(R_2/s) X_m^2}{(R_2/s)^2 + (X_2 + X_m)^2} \right)^2 + \left( X_1 + \frac{X_m \left( (R_2/s)^2 + X_2(X_2 + X_m) \right)}{(R_2/s)^2 + (X_2 + X_m)^2} \right)^2} \quad (15)$$

$Z_{in}$  is updated after every computation step, as  $I_m$  and hence  $X_m$  are updated.

The above procedure is applied in the range from stand-still to the pull-out point, which is described as the unstable operating region of the torque-speed characteristic. The stable operating region of the torque-speed characteristic is the portion corresponding to range from the no-load speed (the synchronous speed) to the pull-out speed.

Equations (9) converge to correct values in the range from stand-still to pull-out point. No convergence is achieved when speed exceeds the pull-out speed, which identifies the pull-out slip  $s_{po}$ , pull-out torque  $T_{po}$ , and hence the pull-out speed  $n_{po}$ . These values will be used for rapid calculation of the performance in the stable operating region as will be explained in the following section. This also identifies the limit between the stable and unstable operating regions on the speed-torque characteristic. These values are used as the starting point for the solution to be obtained for the stable operating region of the torque-speed characteristic.

In the stable operating region of the torque-speed characteristic, i.e., the region of the torque-speed characteristic between the pull-out speed and synchronous speed, the torque decreases sharply as the speed increases. Therefore the procedure described above can not be applied in the stable operation region of the torque-speed

characteristic, as decreasing the torque in above equations, will repeat itself towards the lower torque values, on the unstable region of the torque-speed characteristic. In fact different eigenvalues are dominating the solutions in the stable and unstable operating regions. Therefore between the pull-out point and synchronous speed, another simple procedure, which is described below is used.

In constant current operation the speed regulation is very small in the range from pull-out speed to synchronous speed, i.e., in the stable operating region. Hence in this range the speed-torque characteristic is almost a linear relation between torque and speed, and with a negligible error, the speed-torque relation can be expressed as [8]:

$$n = n_s - \frac{(n_s s_{po})}{T_{po}} T_L \quad (16)$$

Hence, slip  $s$  can be expressed as [8]:

$$s = \frac{s_{po}}{T_{po}} T_L \quad (17)$$

Where pull-out slip  $s_{po}$  and pull-out torque  $T_{po}$  are obtained as described above. Since after this step the slip is known as in terms of the load torque, as given in Equation (17), then the only unknown to be determined in the stable operating region is the magnetizing reactance  $X_m$ . In this case using the torque equation given in Equation (3) together with Equation (17),  $X_m$  can be computed directly as:

$$X_m = \sqrt{\frac{(R_2 T_{po} / s_{po})^2 \omega_s}{3 (R_2 T_{po} / s_{po}) I_d^2 - \omega_s T_L^2}} \quad (18)$$

The input voltage of the motor again computed using Equation (14).

In CSI fed induction motors with terminal capacitors that are used filtering out the voltage spikes resulting from switching of inverter elements, the magnetizing flux and the terminal voltage of the motor is almost sinusoidal. Also since only two inverter switching devices are conducting at a time, two stator phases of the motor are sharing the dc link voltage, which is the output voltage of the input rectifier. Therefore the rms value of the output voltage of rectifier will be equal to the rms line-to-line voltage of the motor, which is the voltage that has been already calculated by using Equation (14). Hence having obtained the required motor input voltage, a relation can be established between the input voltage and the rectifier firing angle  $\alpha$ , by equating the rms value of the rectifier output voltage to the rms line-to-line voltage across the motor terminals. Therefore following relation can be established:

$$\alpha = \frac{1}{2} \arccos \left( \sqrt{\frac{2\pi}{3\sqrt{3}} \left( \left( \frac{V_m}{V_{in}} \right)^2 - 1 \right)} \right) \quad (19)$$

Where  $V_{in}$  is the rms value of the line-to-line supply voltage feeding the rectifier. Equation (19) also, indirectly, gives the relation between the rectifier firing angle and the load torque.

Equation (19) is obtained using the well known relation between the input voltage and rms output voltage of a three-phase full wave controlled rectifier operating under

continuous current conduction mode. Therefore with the firing angle values adjusted according to one which is obtained from Equation (19) the rectifier will always operate under continuous current mode, which is an important advantage, as in such an operating condition harmonics and hence system losses will be reduced significantly as compared to discontinuous current mode of operation under same output power condition.

Information obtained (19) can be a very useful tool in the system analysis and design procedure.

### 3. APPLICATION EXAMPLE

The modeling described in the above section is applied to a 500 kW, 50 Hz, 3300 V, 8 pole cage induction motor, which has equivalent circuit parameters as:  $R_1 = 0.42 \Omega$ ,  $R_2 = 0.58 \Omega$  and  $X_1 = 1.197 \Omega$  and  $X_2 = 1.197 \Omega$ .

Iron losses and the rotor winding leakage reactance are ignored. All parameters are referred to the stator side. A 100 A current source is used, in the following results, which is in value very close the rated current of the motor.

The magnetizing flux linkage of the motor is computed from design details and it is modeled as given in Equation (1). The original flux linkage of the motor is computed from the design details and its model which is given in Equation (1) is compared in Fig. 3. From this figure it is evident that Equation (1) represents the magnetizing characteristic with a high accuracy. The model parameters used in Equation (1) are obtained by curve fitting technique and their values are given below:

$$a_1 = 34.596, a_2 = 0.05844, b_1 = 190.4, b_2 = 8.9196, b_3 = 0.24198, b_4 = 0.00974.$$

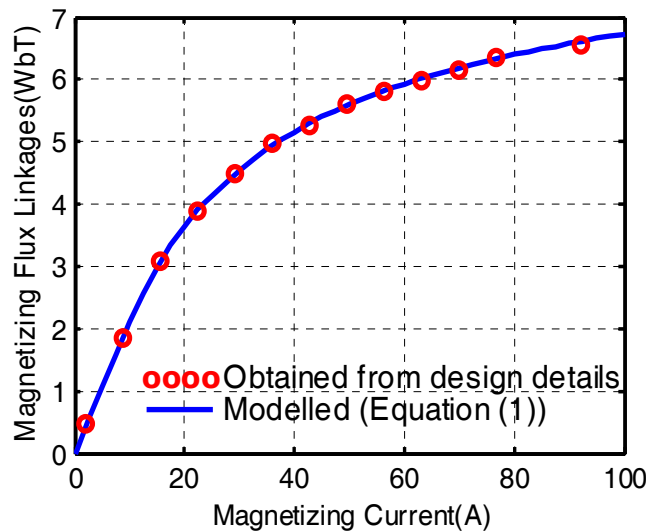


Fig. 3. Magnetizing characteristic of the motor

Using the procedure described in the previous section the motor line-to-line voltage is computed and it is plotted in Fig. 4, against the load torque. It is evident from this figure that, in the unstable operating region the required input voltage varies within large limits. But in the stable operating region (from pull-out speed to synchronous speed) the variation in the input voltage is very small.

The torque-speed characteristic under described operation is given in Fig. 5. As can be seen from this figure that in case of constant current operation the pull-out slip is very small (very small speed regulation) and the torque-speed characteristic is almost linear in this range. Utilizing the solution for unstable region (last converged solution for the unstable region) the pull-out torque and the pull-out speed are obtained as  $T_{po} = 4364$  Nm and  $n_{po} = 729.26$  rpm (which gives  $s_{po} = 0.02765$ ) respectively. These values are used as starting point for the solution obtained for stable operation region.

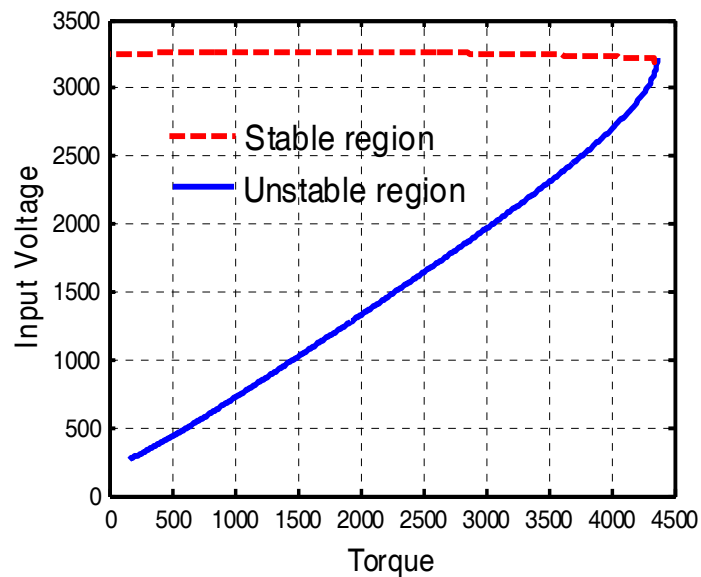


Fig. 4. Variation of required motor input voltage with the load torque

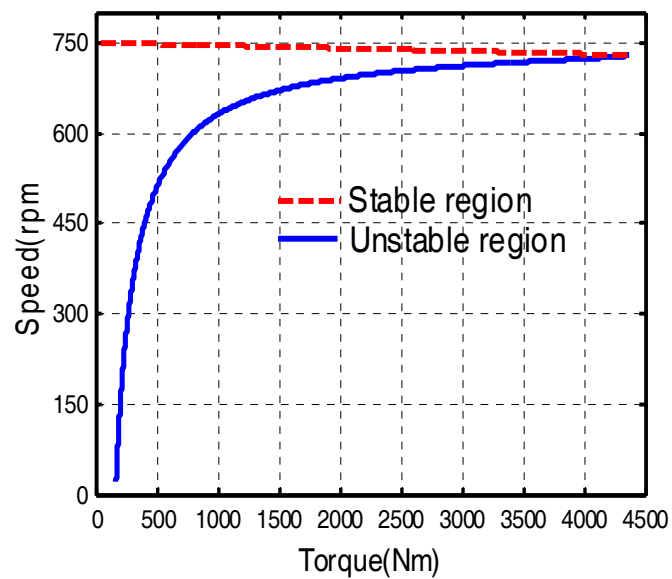


Fig. 5. Speed-torque characteristic

Variation of both the magnetizing and the rotor currents with the load torque are given in Fig. 6. As can be seen from this figure, the magnetizing current is continuously increasing in both stable and unstable regions. In low slip region, the magnetizing current is very large and the rotor current is very low. This is due to the fact that at very low slip region, the load demands very low active power from the motor, and hence the magnetizing current becomes closer to the input current source. In such a case the motor is driven into strong saturation, whereas in the normal voltage source operation (that is motors are normally designed for), the magnetizing current (for relatively large motors such as the one used in this paper) varies between only 10 to 20 % of the rated current of the motor .

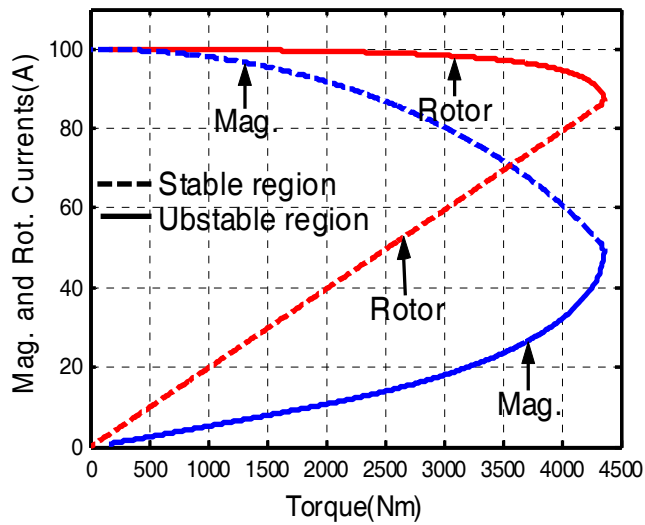


Fig. 6: Variation of magnetizing and rotor currents with load torque

Variation of the rectifier firing angle with the load torque is computed by using (19) and result is illustrated in Fig. 7. As can be seen from this figure there are four distinct sectors for the firing angle as the load torque varies. First three sectors, where rapid changes are observed in firing angle, are for the unstable operating region. Fourth and almost constant firing angle sector is for the stable operating region.

It is evident from Fig. 4 that, in the unstable operating region the required input voltage varies within large limits. But in the stable operating region (from pull-out speed to synchronous speed) the variation in the input voltage is very small. (dashed line sectors in Fig. 4). The three sectors for firing angle in the unstable region correspond to three different values of supply voltage, i.e., rectifier input voltage has to be applied in three different levels. This is because three-phase controlled rectifiers, operating in the continuous current operating mode, the rms value of the rectifier output voltage remains between 42% and 135% of the rms value of the line-to-line supply voltage. Once the required motor input voltage falls out of this band, the supply voltage need to be changed. Therefore to meet the value of the required motor input voltage corresponding to different values of load torque and also to hold the rectifier in the continuous current operating mode, the supply voltage has to be applied in pre-determined steps, for covering the operation in all parts of the unstable operating region. In this investigation the supply voltage steps were pre-determined as 600 V, 1800 V and 3300 V respectively. The last of these supply voltage value is the rated voltage of the motor.

The supply voltage value applicable to the last sector of the unstable region is also valid for the stable operating region.

Magnified plot of firing angle versus load torque in the stable operating region is given in Fig. 8. It is evident from this figure that in the stable operating region the

variation in the firing angle is very small, as the required motor input voltage in this region also varies within very close limits.

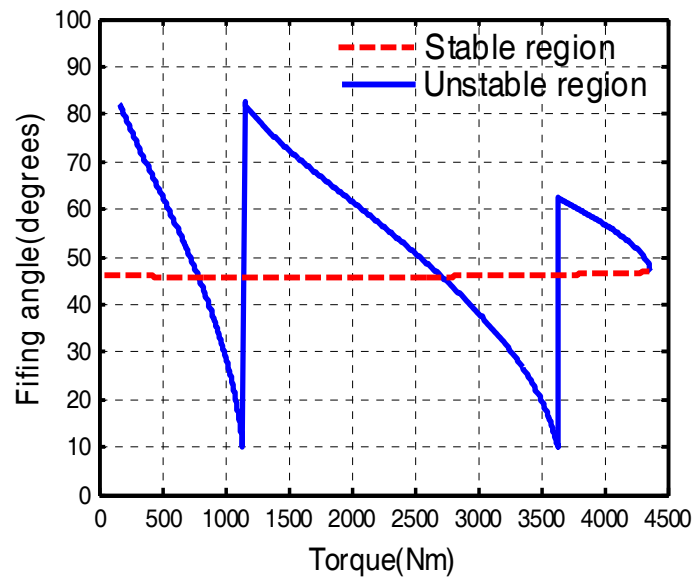


Fig. 7. Input rectifier firing angle versus load torque

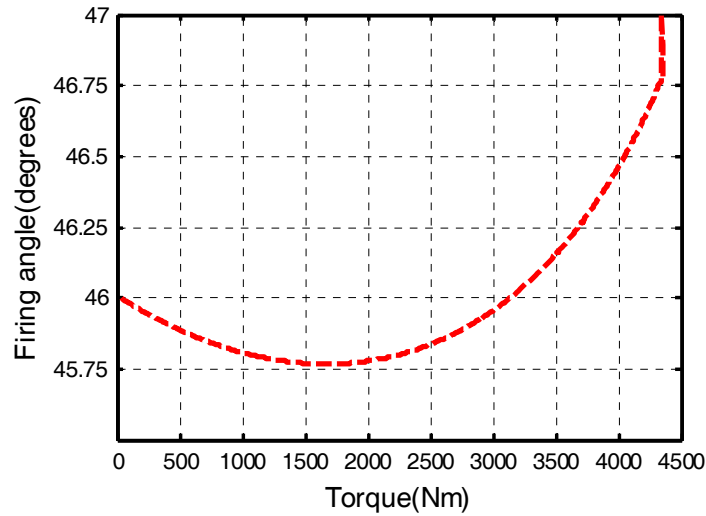


Fig. 8. Magnified version of input rectifier firing angle with load torque for stable operating region

The supply voltage value applicable to the last sector of the unstable region is also valid for the stable operating region.

Magnified plot of firing angle versus load torque in the stable operating region is given in Fig. 8. It is evident from this figure that in the stable operating region the variation in the firing angle is very small, as the required motor input voltage in this region also varies within very close limits.

#### 4. CONCLUSION

In this paper a clear procedure is presented for investigation of the input voltage requirements and corresponding rectifier firing angle of a constant current operated (CSI fed) induction motor, in relation to the variation of the load torque. It is found that for a the speed range from rest to pull-out speed (which is called as unstable operating region) the required motor input voltage and corresponding rectifier firing angle, that insure continuous current operation, varies within large limits as the load torque varies between starting torque to pull-out torque. On the contrary, in the stable operating region, which is defined as the region between the pull-out speed and the synchronous speed, the required motor input voltage and naturally the corresponding rectifier firing angle, which ensure continuous current operation, changes very little. It is sown that in the unstable operating region, in order to meet the motor input voltage requirement and also to hold the rectifier in the continuous current mode of operation, the supply voltage has to be applied in various steps, which can be pre-determined using procedure developed in this paper.

It is clearly demonstrated that the rectifier firing angle corresponding to a given load torque can be easily determined.

It is believed that the information presented in this paper can be very useful in system analysis and design stages.

### 5. REFERENCES

1. P. Vas, Electric Machines and Drives, A space vector approach, *Clerendon Press, Oxford, 1996*.
2. E.P. Cornel, and T.A. Lipo, Modeling and design of controlled current induction motor drive system, *IEEE Trans. on Ind. Appl.* **IA-13**, 321-331, 1977
3. G.K. Creighton, Current source inverter fed induction motor pulsations, *Proc. IEE, Pt. B*, **127**, 231-239, 1986.
4. S. Juvarayan, R. Belamkonda and V. Subrahmanyam, Analysis of a current controlled inverter-fed induction motor drive using digital simulation, *IEEE Trans. on Industrial Electronics and Control Instrumentation*, ECI, **27(2)**, 67-76, 1986.
5. H.G. Kim, S.K. Sul and M.H. Park, Optimal efficiency drive of a current source inverter fed induction motor by flux control, *IEEE Trans. on Ind. Appl.*, **IA-20**, 1453-1459, 1984.
6. H. Kim and M.T. Jahns, Current control for ac motor drives using a single DC link current sensor and measurement voltage vectors, *IEEE Trans. on Ind. Appl.*, **42**, 1539-1547, 2006.
7. S.C. Chapra and R.P. Canale, Numerical Methods for Engineers, fifth edition, *McGraw Hill, NY*, 2006.
8. M. Akbaba, Lecture Notes on Electric Drives, University of Bahrain, 2002.